Alexandria Engineering Journal (2021) 60, 5175–5181

Alexandria University

Alexandria Engineering Journal

www.elsevier.com/locate/aej
www.sciencedirect.com

Transient discharge characteristics of insulator short-circuit under high voltage

Shancheng Qi [a], **Shuaibing Chang** [a,*], **Lilu Cao** [b]

[a] *School of Electrical Engineering and Automation, HeNan Institute of Technology, Xinxiang 453003, China*
[b] *XJ Group Corporation, Xuchang 461000, China*

Received 23 February 2021; revised 29 March 2021; accepted 6 April 2021

KEYWORDS

Insulator short circuit;
High voltage discharge;
Partial discharge;
Short-circuit fault;
Numerical simulation

Abstract The insulation failure is common in high voltage transmission. Based on experimental structure, this paper adopts the finite element method to establish the mathematical model of the short-circuit insulator discharge. Simplify the insulator discharge into a short circuit process between the upper and lower plates, and explore the process of generation, adsorption and neutralization of electrons, positive ions and negative ions, studied how the space charge variation affects the electric field intensity, and analyzed the distribution of each type of ionization products from the wires during the discharge. The results show that: when the insulator is short-circuited and discharged, the area with larger electric field strength is mainly concentrated near the upper plate; the electric field intensity in the discharge space tended to stabilize at the completion of the discharge; when the short-circuit wires were fused, the electron concentration remained stable for a short while at certain positions of the discharge space; as the discharge continued, the electron concentration at these positions declined rapidly; the electrons moved to the plates, causing fluctuations in electric field intensity; the variation of electron concentration during the discharge obeyed the Gaussian distribution. The research results provide the experimental evidence and theoretical reference for avoiding transient discharge in equipment operation.

© 2021 THE AUTHORS. Published by Elsevier BV on behalf of Faculty of Engineering, Alexandria University. This is an open access article under the CC BY-NC-ND license (http://creativecommons.org/licenses/by-nc-nd/4.0/).

1. Introduction

Recent years has witnessed rapid development of new energy technology in China. Wind power occupies a large share of new energy. However, wind farms are usually located in remote areas with harsh environments [1,2]. It is very difficult to transmit the generated power from the wind farms to consumers. Transmission failures often occur in windy weather.

Insulator failure is one of the most frequent transmission failures [3]. This failure mostly manifests as partial discharge, such as surface discharge, coating discharge, internal discharge, and corona discharge. Partial discharge may occur in any insulating medium or hybrid insulation of multiple media. The main sources of partial discharge include voids, cavities, and air bubbles in liquid or solid–liquid insulation, as well as sharp particles or edges in the insulation. If it occurs in

* Corresponding author.
E-mail address: shuaibing_chang@163.com (S. Chang).
Peer review under responsibility of Faculty of Engineering, Alexandria University.

https://doi.org/10.1016/j.aej.2021.04.028
1110-0168 © 2021 THE AUTHORS. Published by Elsevier BV on behalf of Faculty of Engineering, Alexandria University.
This is an open access article under the CC BY-NC-ND license (http://creativecommons.org/licenses/by-nc-nd/4.0/).

liquid-impregnated paper, partial discharge [4] will produce bubbles that induce even more partial discharges.

Unlike other partial discharges, corona discharge is visible and gives off a hissing sound. When the electric field is sufficiently strong, the gas could be ionized to cause electrical breakdown. Then, bubbles will form in gas-filled voids, because the gas has a smaller dielectric constant than the materials surrounding the void. Once the tangential electric field is strong enough to electrically break down the surface [5], surface discharge will occur. In addition, corona discharge could take place in the parallel gaps between insulators, if electrical equipment is switched incorrectly, or if the environment conditions change abruptly. Then, the electrical equipment will fail, and result in safety hazards. To prevent operating risks of equipment, it is very important to avoid the surface discharge of the insulator from polluting the surface. Therefore, the discharge law when the insulator is short-circuited is analyzed through experiments or numerical methods.

High-voltage discharge [6] is a complex physical process. Although capable of disclosing the physical nature of the process, physical experiments face a high instrument cost, and have difficulty in revealing the internal characteristics of high-voltage discharge. With the continuous development of mathematical modeling and computer technology, many scholars have resorted to numerical methods to study the corona discharge [7–11]. For example, Zhang et al. [12] constructed a calculation model for two-dimensional (2D) direct current (DC) calculation model, and compared the calculated results with the data obtained from experiments. Simaet al. [13] combined the continuity equation of charged particles with the electron energy balance equation into the creeping discharge model for nitrogen/oxygen plasma creeping discharge, and verified the rationality of the model by analyzing the surface charge density distribution observed in experiments. Othman et al. [14] used the finite element method to study the space charge distribution in the vicinity of the contaminated insulator in the transmission line and the characteristics of the current pulse during discharge. The numerical calculation results are basically consistent with the experimental results. Wu [15] proposed a corona discharge model based on fluid mechanics, and added multiple ionization equations to realize the microscopic analysis of DC corona discharge. Based on the drift–diffusion equation and Poisson's equation, Gao et al. [16] constructed a numerical model for point-plate discharge model, and compared the features of pulse current under the voltage of 24–27 kV, providing a reference for sensitivity analysis on pulse parameters to these features.

Air discharge is an extremely complex problem. The research on equipment failure caused by partial discharge is mainly limited by calculation efficiency, considering the complexity of corona discharge and the huge computing load [17], this paper builds a discharge model through the COMSOL, aims to study the macroscopic discharge process when the insulator is short-circuited. To improve calculation efficiency, the types of substances generated by the discharge were simplified into three types: electrons, positive ions, and negative ions, regardless of the arc exothermic process during the discharge process. Meanwhile, our model considers the electric field changes caused by variation in space charges. Admittedly, the simplified model cannot fully describe the air ionization induced by the arc from the short-circuited insulator. But the model provides an important tool to study insulator failure, and reveals the distribution law of the three kinds of substances during the discharge.

2. Mathematical model

By Poisson's equation, the electric field intensity [18] can be described as:

$$E = -\nabla V \tag{1}$$

$$\nabla \cdot E = \frac{\rho}{\varepsilon_0} \tag{2}$$

where, E is the spatial vector of the electric field, (V/m); V is the potential at the spatial position (x, y, z), (V); ρ is the space charge density, (C/m^3); ε_0 is the vacuum dielectric constant, (F/m).

This paper mainly considers the high-voltage discharge process of insulators. Therefore, the effect of fluid on electron migration was neglected.

The solution of electron migration and diffusion, electron density and average electron energy directly affects the space charge density and electron distribution law.The above key parameters are described by equations as follows:

$$\frac{\partial}{\partial t}(n_e) + \nabla \cdot [-n_e(\mu_e \cdot E) - D_e \cdot \nabla n_e] = R_e \tag{3}$$

$$\frac{\partial}{\partial t}(n_\varepsilon) + \nabla \cdot [-n_\varepsilon(\mu_\varepsilon \cdot E) - D_\varepsilon \cdot \nabla n_\varepsilon] + E \cdot \Gamma_e = R_\varepsilon \tag{4}$$

The electron diffusivity and mobility involved in the above equations, as well as the electron energy diffusivity, can be expressed by equations as follows:

$$\begin{cases} D_e = \mu_e T_e \\ \mu_\varepsilon = \frac{5}{3}\mu_e \\ D_\varepsilon = \mu_\varepsilon T_e \end{cases} \tag{5}$$

Let M and P be the number of reactions that cause changes to electron density, and that cause neutral collisions between inelastic electrons, respectively.

Then, the source term of electron density can be expressed as:

$$R_e = \sum_{j=1}^{M} x_j k_j N_n n_e \tag{6}$$

Among them, x_j is the mole fraction of reactant j; k_j is the velocity coefficient of reactant j ,(m^3/s); N_n is the total neutral number density, ($1/m^3$).

There is energy consumption in the process of electron migration and diffusion. This energy consumption can be considered as the sum of the collision energy consumption of all reactions:

$$R_e = \sum_{j=1}^{P} x_j k_j N_n n_e \Delta\varepsilon_j \tag{7}$$

Among, $\Delta\varepsilon_j$ is the energy consumption of reaction j, (eV). The velocity coefficients can be obtained by integrating the cross-sectional data:

$$k_k = \gamma \int_0^\infty \varepsilon \sigma_k(\varepsilon) f(\varepsilon) d\varepsilon \tag{8}$$

Among, $\gamma = (2q / m_e)^{1/2}$ ((C/kg)$^{1/2}$); m_e is the electron mass, (kg); ε is energy, (eV); σ_k is the collision cross section, (m^2); f is the distribution function of electron energy.

The mass fraction of non-electronic substances can be described as:

$$\rho \frac{\partial}{\partial t}(w_k) + \rho(u \cdot \nabla)w_k = \nabla \cdot j_k + R_k \tag{9}$$

As the charged substance moves, the space charge density will change with the charge migration. Therefore, the relationship between the space charge density and the discharge product before can be expressed by formula (10):

$$-\nabla \cdot \varepsilon_0 \varepsilon_r \nabla V = \rho \tag{10}$$

3. Simulation model

3.1. Model definition

Fig. 1(a) illustrates the discharge process of the test insulator. During the experiment, the short-circuit fault was simulated by connecting the upper and lower plates with an ultrathin wire, since the insulator discharge process is mainly caused by air breakdown, the calculation model constructed in this paper ignores the influence of wire size on the discharge. As shown in Fig. 1(b), the test structure has two dimensions. Since the discharge takes place instantaneously, the areas near the plates and wires were meshed into denser grids, making the computation more accurate. In actual scenarios, the short-circuited wires will fuse immediately under high voltage. Therefore, a function was designed to control the action time of the wires in the computing process. Fig. 1(c) is the calculation grid. This article focuses on the discharge characteristics of the short-circuit area. Therefore, the grid in this area is refined.

3.2. Boundary conditions and correlation coefficients

The upper plate was loaded with a voltage of 580 kV, while the lower plate was grounded. The discharge process was regarded as a continuous ion reaction. The background gas, air A, can be ionized into positive ions, negative ions, and electrons. The specific reactions are shown in Table 1.

Due to the influence of electric field force, the positive ions move and neutralize near the lower plate. Thus, the concentration of positive ions was set to zero at the lower plate. For similar reasons, the concentration of negative ions and electrons was set to zero on the surface of the upper plate. The other boundaries were regarded as zero flux boundaries.

This research mainly targets the discharge breakdown process of the upper and lower plates of the insulator. Therefore, the computational object was simplified as the upper and lower plates connected by wires, and the discharge was assumed to complete once the wires are discharged and fused. Therefore, Gaussian pulse function was added to the wire boundary to mimic the fusion effect of instantaneous discharge, the characteristics of ion migration and diffusion were studied by comparing and analyzing the concentration distribution of reaction products in discharge space.

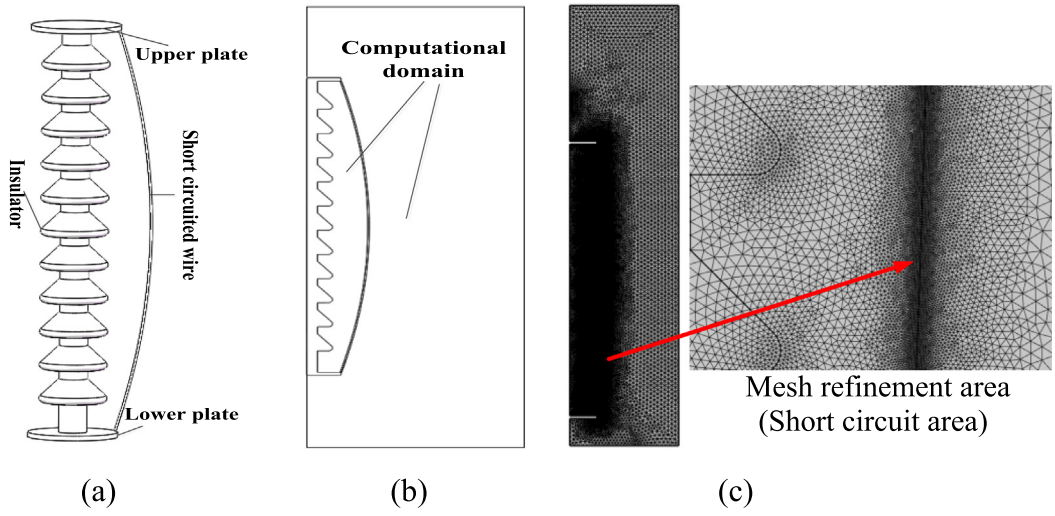

Fig. 1 Insulator short-circuit model.

Table 1 Collisions and reactions.

Reaction	Formula	Type	$\Delta\varepsilon$ (eV)	k_f (m^3/s)
1	$e + A => p + 2e$	Ionization	15	–
2	$e + A => n$	Attachment	–	–
3	$e + 2A => n + A$	Attachment	–	–
4	$e + p => A$	Reaction	–	$5*10^{-14}$
	$n + p => 2A$	Reaction	–	$5*10^{-12}$

4. Results analysis

4.1. Distribution of electric field

The distribution of the spatial electric field intensity at 10 ns is presented in Fig. 2, where the arrows indicate the direction of electric field vectors. It can be seen that the area with larger electric field intensity is mainly concentrated at the right edge of the upper plate. This is because tip discharge is easy to occur at this geometric tip with a small radius of curvature. Thus, the corona arc is first excited at the edge of the upper plate, immediately after the wires are connected.

Fig. 3 shows the curves of the electric field intensity corresponding to the positions of the edge vertices of upper and lower plates. It can be seen that the electric field intensities at the edge vertices of the two plates changed with the development of the discharge; the electric field at an edge vertex of the upper plate was much more intense than that at the corresponding edge vertex of the lower plate. The reason is that the upper plate is loaded with high voltage. At the moment of electrification, the electric field intensity at this plate increased rapidly, sparking corona discharge. Then, the charged substances (electrons, positive ions, and negative ions) were rapidly ionized, and went through anisotropic electrode migration. According to formulas (1) (2) and (10), the movement of these substances will change the electric field intensity. When the wires are fused, the charged substances will be neutralized at the two poles, causing the field intensity to stabilize. As shown in Fig. 3, the electric field intensity dropped rapidly after reaching the peak.

4.2. Distribution of electron concentration

Fig. 4 shows the distribution of electron concentration at each moment. It can be seen that, when the wires conducted electricity, the electron concentration of the upper plate immediately dropped to the lowest point. As time progressed, the electron concentration in the computational domain started to fall below the initial concentration, for the electrons continuously migrate and neutralize to the electrode plates. When the wires were fused, the circuit no longer released electrons, and the released electrons were basically neutralized in motion, under the action of the electric field. Since the electrons in the computational domain were mainly released around the wires, the low concentration area of electrons near the upper plate continued to expand.

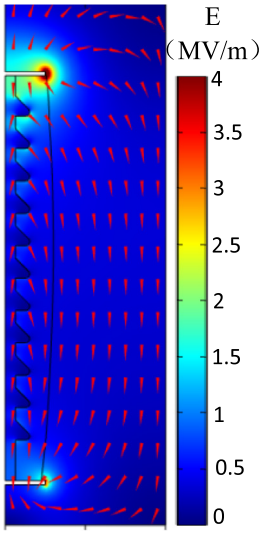

Fig. 2 Distribution of electric field intensity at 10 ns.

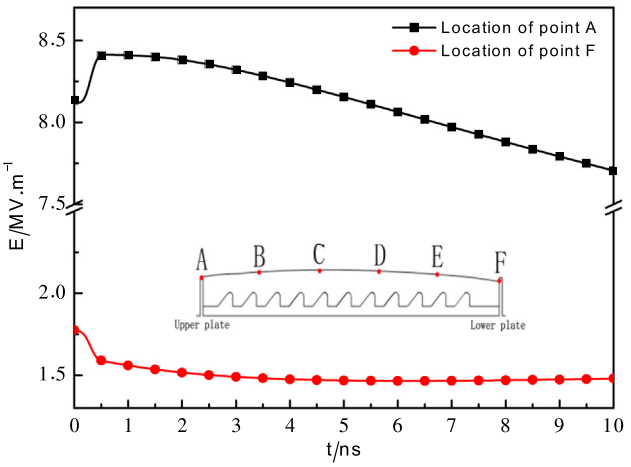

Fig. 3 Electric field intensity at the edge of the upper and lower plates.

Fig. 5 shows the variation of electron concentration at six points on the wires, from the discharge of the insulator to the fusion of the wires. It can be seen that, the electrons were excited instantly as the insulator was short-circuited and discharged, resulting in a sharp rise in electron concentration. The electron concentration was particularly high near the middle of the short circuit. During the discharge, electrons moved to the upper plate under the influence of the electric field effect. Due to the adsorption and neutralization at the upper plate, the electron concentration on that plate approached the initial concentration. In the meantime, the electron concentration at other positions increased, and started to descend at the completion of the discharge. It is easy to infer that the electron concentration during the discharge maximized at about 0.5 ns.

To better understand the distribution of discharge products between upper and lower plates, the lower plate was taken as the start point and the lower plate as the end point along the short-circuit wires. Then, the product concentration at the critical moment in the discharge process is presented in Fig. 6. It can be seen that, a stable concentration area appeared on the wires from the discharge of the insulator to the fuse of the wires. After the discharge was completed, this stable concentration area began to shrink. This is because a large amount of plasma is generated near the wires as they are fused. The plasma continuously ionizes gas molecules,

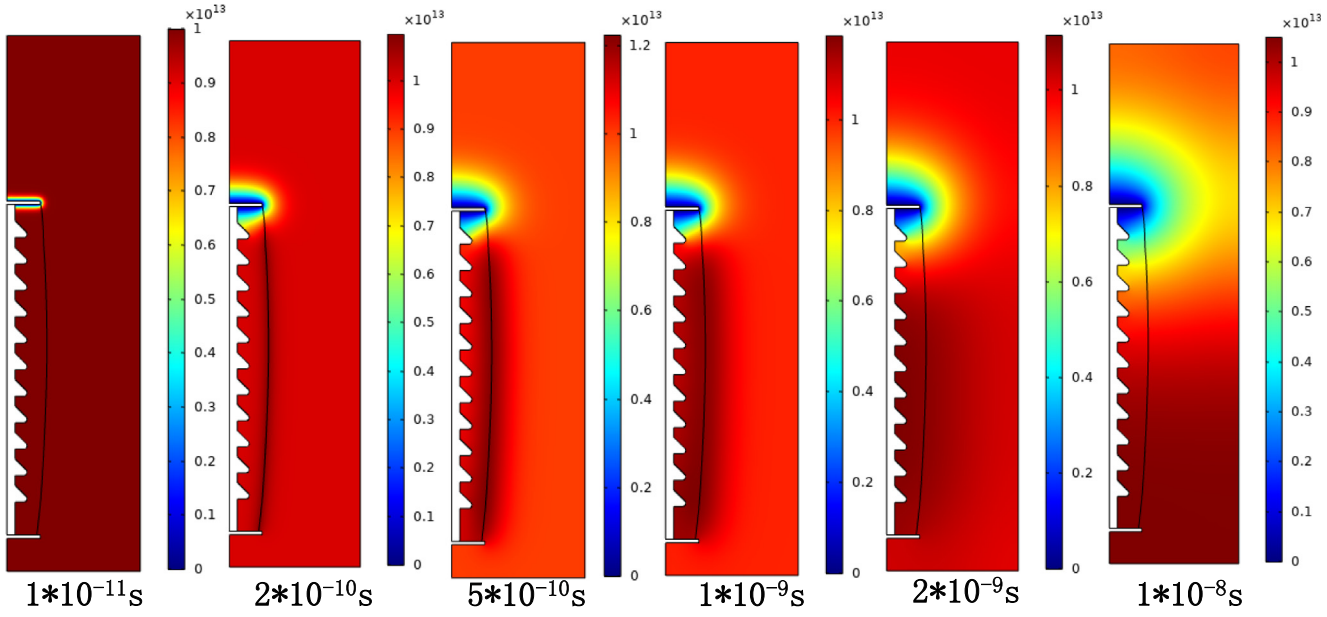

Fig. 4 Distribution of electron concentration.

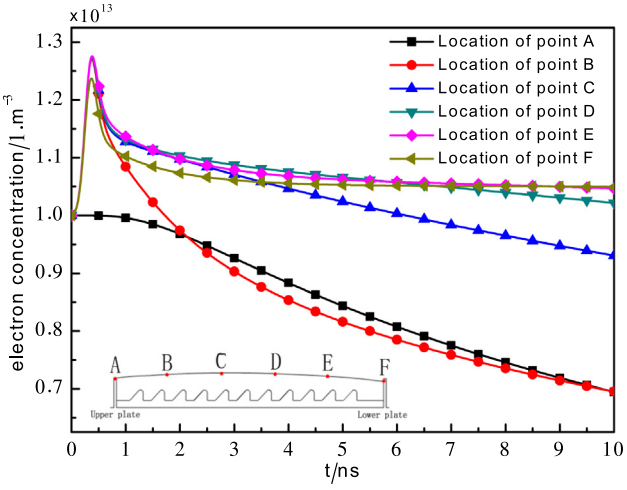

Fig. 5 Variation of electron concentration with time.

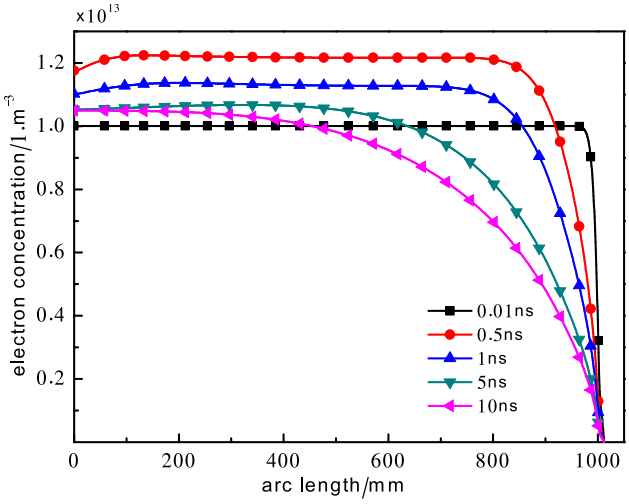

Fig. 6 Variation of electron concentration along short-circuited conductor.

and stabilizes the concentration of ionized products. In engineering, it is necessary to avoid such a continuous discharge process.

4.3. Distribution of space charge density

Fig. 7 shows the distribution of the space charge density at each time. This paper mainly investigates the short-circuit discharge caused by positive high voltage. Thus, the space charge density near the wires was initially negative. At the moment of electrification, the space charge density in the vicinity of the wires started to increase. When the wires were fused at 0.5 ns, the discharge induced by short circuit came to a stop, and the space charge gradually moved to the two plates and got neutralized.

Fig. 8 shows the change of the space charge density at various points along the wires with the elapse of time. The results show that the space charge density of the upper plate exhibited positive charge fluctuations at the moment of discharge. A possible reason is that the upper plate is at a positive high voltage, and the electrons are instantly neutralized at the moment of discharge. Meanwhile, the remaining positive ions begin to migrate to the lower plate, making their space charge positive. When the other positions are discharged, lots of electrons and negative ions do not migrate to the positive electrode. That is why the space charge is negative at these positions during the discharge. With the termination of the discharge, the electrons and negative ions at these positions move to the upper plate and get neutralized. Hence, the space charge density eventually tends to stabilize.

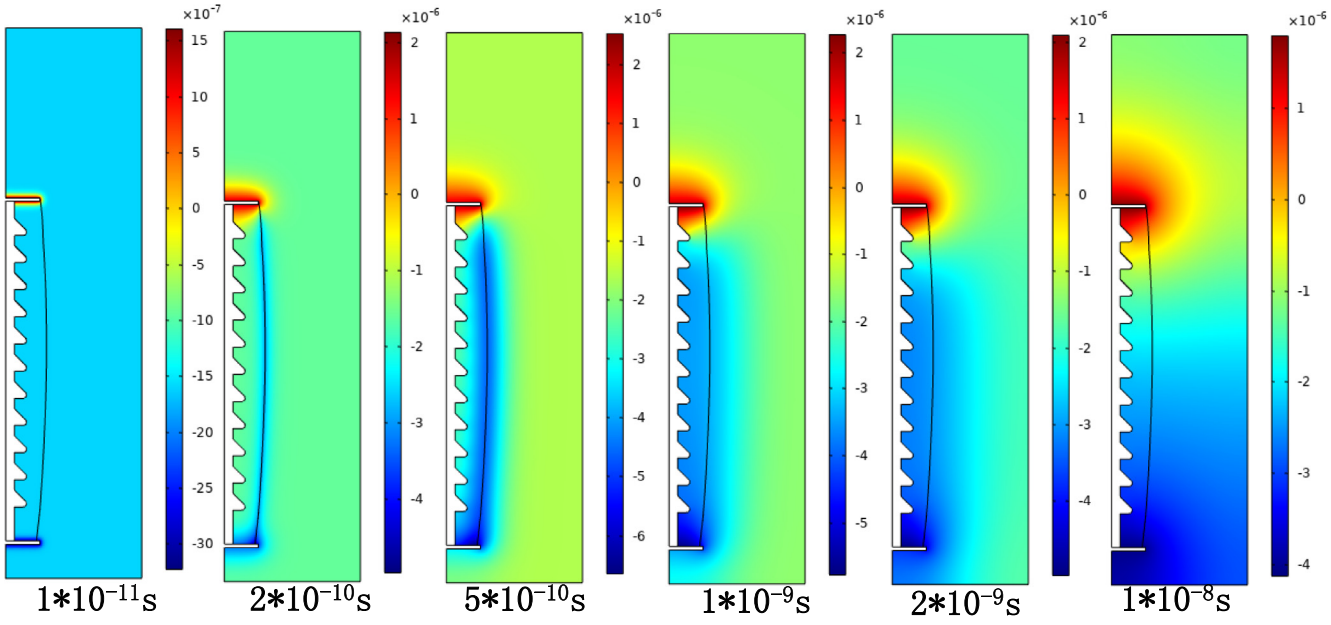

Fig. 7 Variation of space charge density at each time.

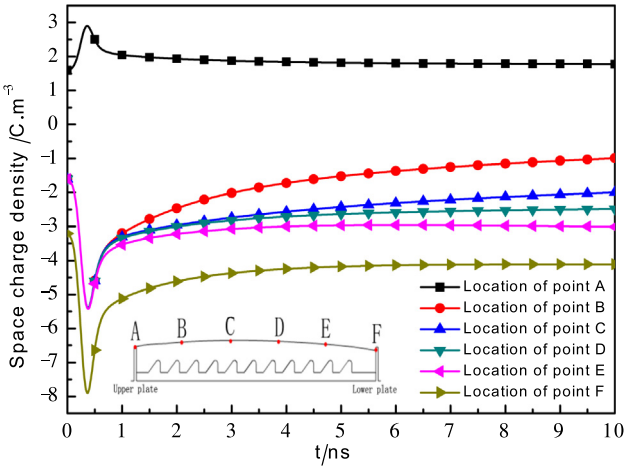

Fig. 8 Variation of space charge density at each time.

5. Conclusions

This paper designs an experimental structure to study the short-circuit discharge characteristics of insulators, and numerically simulates the process from short-circuit discharge of insulators to wire fusion, providing a theoretical reference for the research into insulator discharge. The main conclusions are as follows:

(1) The electric field intensity near the upper plate was relatively large during the discharge process, and the electric field intensity in the discharge space tended to stabilize at the completion of the discharge. These observations verify the effect of space charge on electric field intensity.

(2) When the short-circuit wires were fused, the electron concentration remained stable for a short while at certain positions of the discharge space. As the discharge continued, the electron concentration at these positions declined rapidly. The electrons moved to the plates, causing fluctuations in electric field intensity.

(3) The short-circuit fault of insulators was simplified as the short circuit of the wires between the two plates. The fusion process of the wires was regarded as the release of Gaussian pulse. The results show that the variation of electron concentration during the discharge obeyed the Gaussian distribution.

Declaration of Competing Interest

The authors declared that there is no conflict of interest.

Acknowledgement

This work is supported by Henan Institute of Technology High-level Talent Research Startup Fund (KQ1854), Key Science and Technology Projects of Henan Province (202102210208).

References

[1] S. Wang, Analysis of impact on safety operation of wind generating set by natural environment, J. Safety Science Technology 5 (6) (2009), 214e8.

[2] X.P. Yang, X.Y. Liu, G.Y. Kou, C.X. Xu, W.H. Zhang, R. Hu, C. Wang, Z.Y. Zhao, Wind turbine lubrication based on parallel control of multiple factors, J. Européen Systèmes Automatisés 53 (5) (2020) 653–660.

[3] H. Xu, Z.Q. Wang, K. Wang, F.R. Zhou, Y.T. Jiang, Q.J. Peng, Z.X. Lu, Simulation Analysis of Guano Whereabouts Transmission Line Insulator Surrounding Electric Field

Distribution, Science Technology Engineering 15 (14) (2015) 171–175.
[4] X. Wu, Y.J. Ye, Engineering technology development, The status of partial discharge detection in power transformers: Full version 2016 (8) (2016) 206–207.
[5] C.X. Pan, K. Wang, G.Y. Shi, Z.H. Li, Effect of Moisture on the Breakdown Characteristics of Paper Board under AC and DC Voltage, Sci. Technology Eng. 16 (30) (2016) 231–235.
[6] M. Hao, R.B. Liu, M.M. Wang, Q. Lin, Investigation on Power Consumption Characteristics of Spark Discharge Plasma Jet, Science Technology Engineering 15 (4) (2015) 226–228.
[7] C. Zheng, X. Zhang, Z. Yang, C. Liang, Y. Guo, Y. Wang, X. Gao, Numerical simulation of corona discharge and particle transport behavior with the particle space charge effect, J. Aerosol Sci. 118 (2018) 22–33.
[8] R.V.K. Kumar, G.M. Naik, G. Murali, Wireless nano senor network (WNSN) for trace detection of explosives: The case of RDX and TNT, Instrumentation Mesure Metrologie 18 (2) (2019) 153–158.
[9] D.N. Saleh, Q.T. Algwari, F.K. Amoori, Numerical Simulation of the Trichel-Pulse in SF 6 at Atmospheric Pressure, IEEE Trans. Plasma Sci. 47 (1) (2018) 427–433.
[10] P. Marčiulionis, Analysis of space charge distribution in dc corona discharge field computed with finite-element method, IEEE Trans. Plasma Sci. 45 (7) (2017) 1698–1703.
[11] S. Mantach, K. Adamiak, A double-vortex EHD flow pattern generated by negative corona discharge in point-plane geometry, J. Electrostat. 93 (2018) 118–124.
[12] B.L. Zhang, Y.T. Wang, Y.W. Li, Numerical simulation and experimental study for low-pressure direct-current glow discharge, High Voltage Engineering 42 (3) (2016) 724–730.
[13] W.X. Sima, C.X. Liu, M. Yang, Plasma model of gas discharge along the dielectric surface, Proc. CSEE 37 (9) (2017) 278–287.
[14] N.A. Othman, M.A.M. Piah, Z. Adzis, Space charge distribution and leakage current pulses for contaminated glass insulator strings in power transmission lines, IET Gener. Transm. Distrib. 11 (4) (2017) 876–882.
[15] Wu, F.F. (2014). Microphysical process and ion flow field analysis of corona discharge on HVDC transmission lines, Chongqing University, 2014.
[16] Q. Gao, C. Niu, K. Adamiak, A. Yang, M. Rong, X. Wang, Numerical simulation of negative point-plane corona discharge mechanism in SF6 gas, Plasma Sources Sci. Technol. 27 (11) (2018) 115001.
[17] R.Z. Wang, Z.H. Chen, Z.G. Su, Z.S. Zhou, L. Guan, Y.F. Zhang, On the Propagation of Lightning Wave Considering Impulse Corona with Insulation Flashover Model and Tower Model, Science Technology Eng. 15 (7) (2015) 85–91.
[18] L. Vala, P. Chvatal, The mechanism of layer formation from charged powder particles, J. Electrostat. 22 (3) (1989) 289–307.